Global Journal of Engineering and Technology [GJET].
ISSN: **2583-3359** (Online)
Frequency: Monthly
Published By GSAR Publishers
Journal Homepage Link- https://gsarpublishers.com/journal-gjet-home/

First-Principles studies of Mechanical moduli and Thermodynamic Trends of R3̄m $LiCoO_2$ under Pressure

By

D. Yabwa[1,*], M. A. Abdullazeez[2], W. F. Burari[3] and A. M. Tijjani[3]
[1]Department of Physics, Taraba State University, Jalingo, Nigeria
[2,3]Department of Physics, Faculty of Science, Abubakar Tafawa Balewa University, Bauchi, Nigeria

Article History

Received: 11/08/2026
Accepted: 24/08/2026
Published: 26/08/2026

Vol – 5 Issue – 8

PP: - 58-64

Abstract

Rhombohedral $LiCoO_2$ (R3̄m) remains a benchmark layered cathode, yet its long-term cycling life is fundamentally restricted by chemo-mechanical degradation and thermal stresses. To evaluate these structural limits without electronic bias, this study provides a comprehensive first-principles evaluation of its complete elastic tensor and thermodynamic stability. Using Density Functional Theory (DFT) within the Quantum ESPRESSO package, calculations were performed using both PBE-GGA and Hubbard-corrected GGA+U frameworks (U_{eff} = 5.6 eV on Co 3d states) to ensure structural precision. Zero-pressure variable-cell optimizations yield stable conventional hexagonal volumes of volumes of 97.37(Å)^3 for PBE and 97.80(Å)^3 for PBE+U. A Birch–Murnaghan fit yields a bulk modulus of 150 -165 GPa with B′ ≈ 4.0 - 4.5. Aggregated stress–strain averages demonstrate a stiff, elastically anisotropic framework defined by a Voigt bulk modulus B_H = 142.97 GPa, shear modulus G_H = 44.98 GPa, and Young's modulus (E) of 122.12 GPa. The calculated Pugh ductility index B_H/G_H = 3.18, and ν = 0.358) confirm high shear ductility alongside stiff intra-planar structural scaling. Utilizing these elastic parameters, the quasi-harmonic Debye model successfully projects a Debye temperature of 680.93 K, mapping out definitive baselines for temperature-dependent vibrational internal energy, heat capacity, and entropy. Ultimately, these pressure-enthalpy configurations and thermo-mechanical indices provide essential physical parameters required to simulate thermal management systems and design failure-resistant layered battery architectures.

Keywords: *Density Functional Theory; LiCoO2 cathode; Quantum ESPRESSO; Thermodynamic trends; Hubbard U correction; Lithium-ion batteries.*

INTRODUCTION

Rechargeable lithium-ion batteries are central to portable electronics, electric mobility, and emerging grid-storage technologies because they store and release energy through reversible lithium insertion and extraction reactions. (Asamoah., et al 2024) In a lithium-ion cell, the cathode is a key component because it largely determines the operating voltage, reversible capacity, thermal tolerance, safety margin, and long-term structural durability of the device (Nitta., et al 2015 & Koech., et al 2024). The gravimetric energy delivered by a cathode is commonly connected to the product of the reversible capacity and average operating voltage; however, high energy density alone is not sufficient for practical operation (Jiao., et al 2023). A useful cathode must also preserve its host framework during repeated lithium extraction and insertion, resist harmful volume change, maintain electronic transport pathways, and avoid mechanical or thermal degradation under operating conditions (Wu., et al 2026)

Layered lithium cobalt oxide ($LiCoO_2$) remains one of the most important reference cathode materials for lithium-ion batteries (Wang., et al 2018). Since the early demonstration of layered $LiCoO_2$ as a high-voltage intercalation cathode, its well-defined α–$NaFeO_2$ structure good structural reversibility over practical lithium compositions, and strong Co–O framework have made it a model system for understanding layered oxide cathode behavior (Tang.et al 2026). In the fully lithiated state, $LiCoO_2$ crystallizes in the rhombohedral R3̄m structure, commonly described using a hexagonal setting with alternating Li layers and edge-sharing CoO_6 octahedral slabs (Osemeikhian, O. 2017). The strength of Co–O bonding, the hybridization between Co 3d and O 2p states, and the separation between transition-metal oxide slabs control the electronic, mechanical, and thermal response of the cathode framework (Gao., et al 2024). The central materials problem is that the same layered arrangement that enables lithium

*Corresponding Author: D. Yabwa

intercalation can also be sensitive to lattice distortion, slab spacing changes, oxygen-layer rearrangement, and stress accumulation (Romanova., et al 2026). During battery cycling, $LiCoO_2$ particles experience lithium concentration gradients, anisotropic strain, surface reconstruction, thermal fluctuations, and micro-crack formation (Patel. A. 2025). These processes reduce cyclic stability and safety even when the equilibrium crystal structure appears stable. Therefore, understanding the intrinsic structural stiffness, compressibility, elastic response, and thermal trends of the $LiCoO_2$ framework is necessary for connecting atomistic bonding with macroscopic cathode reliability (Haq and Lee, 2025).

Hydrostatic compression offers a highly effective theoretical framework for investigating the intrinsic structural, and thermodynamic behavior of $LiCoO_2$ by systematically modifying the crystal lattice (Maran., et al 2024). Such calculations provide fundamental baseline insights into the material's inherent stability and the evolution of its physical properties under varying structural conditions. While mechanical environments in functioning batteries are highly complex governed by dynamic lithium transport, microstructural evolution, defects, and electrode-electrolyte interactions establishing the pure, intrinsic properties of the pristine crystal lattice serves as an indispensable prerequisite for understanding these advanced degradation mechanisms (Wu., et al 2024).

Previous experimental and theoretical studies have shown that layered oxides may undergo structural rearrangements involving slab gliding, changes in oxygen stacking, or transitions between O3-type and O1-type arrangements during strong delithiation or under extreme external conditions (Hu., et al 2019, Choi., et al 2026, Yu., et al 2024 & Shi., et al 2025). High-pressure studies of $LiCoO_2$ have examined compression behavior, Raman modes, and equation-of-state parameters, with reported bulk moduli typically of the order of 10^2 GPa. (Wang., et al 2005, Cococcioni and de Gironcoli, 2005, Dudarev., et al 1998 & Zhou., et al 2004). These studies confirm the importance of pressure-dependent lattice response, but a complete interpretation requires a highly consistent computational approach to systematically separate equation-of-state trends for specific structural branches from an electronic-structure perspective, a primary computational challenge lies in the treatment of localized transition-metal 3d states. Conventional semi-local Density Functional Theory (DFT) often underestimates band gaps and fails to sufficiently localize Co 3d electrons. For stoichiometric $LiCoO_2$, Cobalt is nominally Co^{3+} with a low-spin t_{2g}^6 configuration in the fully lithiated phase. The Hubbard-corrected DFT+U approach is therefore essential to improve the description of Co 3d states and redox energetics Crucially, to avoid over-interpreting mixed exchange-correlation treatments, a direct, parallel comparison between PBE and DFT+U results must be conducted within an identical computational framework for structural optimization (Wang., et al 200, Giannozzi. P 2017 & Perdew., et al 1996)

Despite the large body of literature on $LiCoO_2$, there remains a critical gap for an internally consistent dataset that directly links optimized structure, formation energies, equations of state, pressure-enthalpy trends, elastic averages and Debye-model thermodynamic behaviors. The specific objectives of this manuscript are twofold. First, we establish a comprehensive, unified PBE and PBE+U framework to accurately quantify the intrinsic response of rhombohedral $LiCoO_2$ to volume deformation. Second, we systematically map the resulting pressure-enthalpy and Debye thermal trends to provide a reliable thermodynamic baseline for the rhombohedral phase branch.

By providing this rigorous, concurrent assessment of the rhombohedral $R\bar{3}m$ phase, this work serves as an essential reference library. We report structural optimizations, PBE/PBE+U, formation energies, Birch–Murnaghan equations of state pressure-enthalpy trends, comprehensive elastic averages, and Debye thermodynamic quantities. This systematically derived data clarifies foundational structural-property relationships, paving the way for targeted future multi-phase stability mapping, spin- state evaluations, and full phonon dispersion profiles.

The rest of the paper is structured as follows: In section 2, we describe the full details of DFT computational parameters and the empirical formalism underpinning the thermodynamic profiles and mechanical properties of the material. Section 3 presents a comprehensive results and analysis of the data while important results are summarized in section 4.

Computational Methodology

The initial structure of layered $LiCoO_2$ was modeled in the rhombohedral $R\bar{3}m$ symmetry using the conventional hexagonal setting. All first-principles, self-consistent field calculations were performed using the plane-wave pseudopotential framework implemented in the Quantum ESPRESSO package Exchange-correlation effects were described using the generalized gradient approximation (GGA) (Giannozzi., et al 2020) formulated by Perdew, Burke, and Ernzerh of (PBE) (Perdew., et al 1996). Projector augmented-wave (PAW) pseudopotentials from the standard Quantum ESPRESSO pseudopotential library were utilized to represent the core-valence electron interactions for Li, Co, and O. To maintain strict internal consistency, the PBE and PBE+U descriptions were applied uniformly across the entire dataset without mixing local density approximation (LDA) parameters. The electronic wave functions were expanded in a plane-wave basis set with a kinetic-energy cutoff of 90 Ry, complemented by a charge-density cutoff of 720 Ry to ensure accurate charge density representation. Brillouin-zone integrations were performed using a well-converged $6 \times 6 \times 3$ Monkhorst–Pack k-point mesh. For the Hubbard-corrected (PBE+U) (Raman, 2026) calculations, a localized, effective on-site Coulomb repulsion parameter of U_{eff} = 5.6eV was applied to the Co 3d states, consistent with established literature values for reproducing the experimental electronic band gap and redox potentials of lithiated transition-metal oxides The stoichiometric system was treated within a non-

*Corresponding Author: D. Yabwa

magnetic, low-spin configuration corresponding to the characteristic $t_{2g}^6 e_g^0$ state of Co^{3+}. Ground-state structural optimizations were carried out using variable-cell relaxation at zero external pressure to simultaneously optimize both lattice parameters and internal atomic coordinates. The iterations were systematically continued until the total energy and ionic force convergence thresholds reached a rigorous tolerance of 10^{-6} Ry and 10^{-3} Ry/bohr, respectively.

Table 1: Structural parameters and energy minimizations.

System	*a* (Å)	*c*(Å)	*c/a*	V_{hex} ($Å^3$)	V/Z ($bohr^3$)	E_f (eV/atom)
PBE	2.840	13.940	4.908	97.37	219.03	-
PBE+*U*	2.830	14.100	4.982	97.80	219.99	-0.374
Experimental XRD Hu., et al 2019	2.817	14.052	4.989	96.54	217.17	

DFT+U and Spin-State Treatment

To rectify the self-interaction errors inherent in standard density functional theory and properly localize the strongly correlated Co 3d states, the rotationally invariant Hubbard +U correction was applied following the Dudarev formulation, where $U_{eff} = U - J$. An effective value of U = 5.6 eV (Lambert and Regan, 2023) was adopted, which has been established as highly reliable for mitigating artificial delocalization and reproducing the experimental electronic band gap in structural cobalt oxides. ambient conditions, stoichiometric $LiCoO_2$ features a low-spin $t_{2g}^6 \quad e_g^0$ configuration electronic configuration (S = 0) driven by the strong octahedral crystal-field splitting of the CoO_6 slabs (Er-Rami, 2022).Consequently, the baseline rhombohedral phase was treated as non-magnetic throughout the variable-cell optimizations. While this constrained spin state accurately describes the ground-state properties, it is noting that hydrostatic compression may induce adiabatic spin crossovers or transitions to intermediate- or high-spin configurations. Because the present pressure vs enthalpy and thermodynamic evaluation focuses strictly on the mechanical responses of the baseline rhombohedral matrix, these potential high-pressure magnetic phase transformations were omitted from the total energy calculations and remain a subject for separate, specialized spin-state phase mapping

Equation of State and Pressure–Enthalpy Analysis

The zero-temperature equation-of-state behavior was obtained from the calculated energy–volume relationship. The energy–volume curve was fitted using the third-order Birch–Murnaghan equation of state

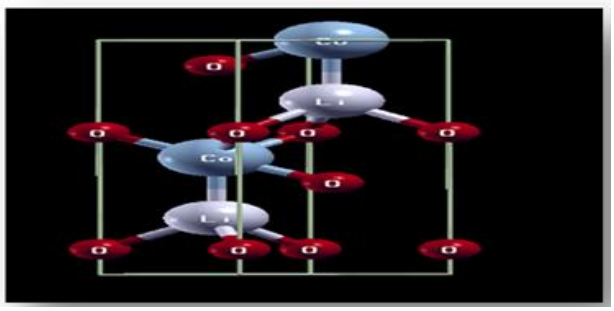

Figure 1. Presents Optimized crystal structures of $LiCoO_2$ compound

$$E(V) = E_0 + \frac{9V_0B_0}{16}\left\{\left[\left(\frac{V_0}{V}\right)^{\frac{2}{3}} - 1\right]^3 - 1\right\}^2\left[6 - 4\left(\frac{V_0}{V}\right)^{\frac{2}{3}}\right] \quad (1)$$

where E_0 is the minimum energy, V_0 is the equilibrium volume, B_0 is the bulk modulus, and B_0' is the pressure derivative of the bulk modulus. The available energy–volume data show a clear minimum near 218–220 $bohr^3$ per formula unit, equivalent to a conventional hexagonal cell volume of approximately 97 $Å^3$ for three $LiCoO_2$ formula units.

The pressure-dependent enthalpy was evaluated from

$$H(P) = E(P) + PV \quad (2)$$

where $E(P)$ is the calculated internal energy along the modeled compression path and PV is the pressure–volume contribution. This calculation describes the enthalpy trend of the rhombohedral $LiCoO_2$ branch.

Elastic and Debye Thermodynamic Calculations

Elastic properties were evaluated using the stress–strain approach implemented through the Thermo PW workflow in Quantum ESPRESSO (Dal-Corso, 2020). The Voigt, Reuss, and Voigt–Reuss–Hill approximations were used to obtain effective isotropic bulk modulus (*B*), shear modulus (*G*), Young's modulus (*E*), Poisson's ratio (*v*), and Pugh ratio (*B/G*).

Temperature-dependent thermodynamic functions were

*Corresponding Author: D. Yabwa

obtained using the Debye model. The Helmholtz free energy was interpreted as

$$F(T) = U(T) - T(S)T \quad (3)$$

where $U(T)$ is vibrational internal energy and $S(T)$ is vibrational entropy. The constant-volume heat capacity is obtained from

$$C_V = \left(\frac{\partial U}{\partial T}\right)_V \quad (4)$$

The Debye model provides an approximate vibrational thermodynamic description and is useful for identifying trends in heat storage, entropy, and free energy

Results and Discussion

Optimized Structure of $LiCoO_2$

The optimized crystal structures of LiCoO2, were obtained by fully relaxing both atomic positions and lattice parameters until the residual forces and total energy converged within the selected thresholds. All compositions retain the rhombohedral structure with space group Layered $R\bar{3}m$, of the overall crystal symmetry of the pristine compound

Table 1 summarizes the optimized lattice parameters and formation energy. The PBE calculation gives a = 2.840 Å, c = 13.940 Å, and c/a = 4.908. The corresponding conventional hexagonal cell volume and is 97.37(Å)^3 equivalent to 32.46 (Å)^{3}per formula unit or 219.03 bohr^3 per formula unit. The PBE+U calculation gives a = 2.830 Å, c = 14.100 Å, and c/a = 4.982, with a conventional hexagonal volume of 97.80 (Å)^3. These volumes are internally consistent with the hexagonal volume relation $V = (3/2)\, a^2 c$.

Formation Energy and Scope of Thermodynamic Stability

The calculated formation energy of $LiCoO_2$ is −0.374 eV/atom within the elemental reference scheme used in the calculations. The negative value indicates that the modeled compound is energetically favorable with respect to the selected elemental references (Rahman., et al 2026).

Equation of State and Compressibility

The calculated energy–volume curve shown in figure 2(a) has the expected parabolic shape around equilibrium, with a well-defined minimum near 218–220 bohr^3 per formula unit. Expressed in conventional hexagonal-cell units, this corresponds to approximately 97 Å^3 for the three-formula-unit cell.

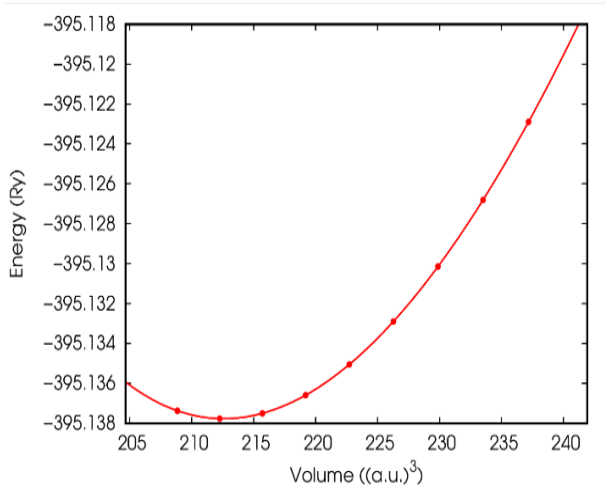

Figure 2(a) Equation of state

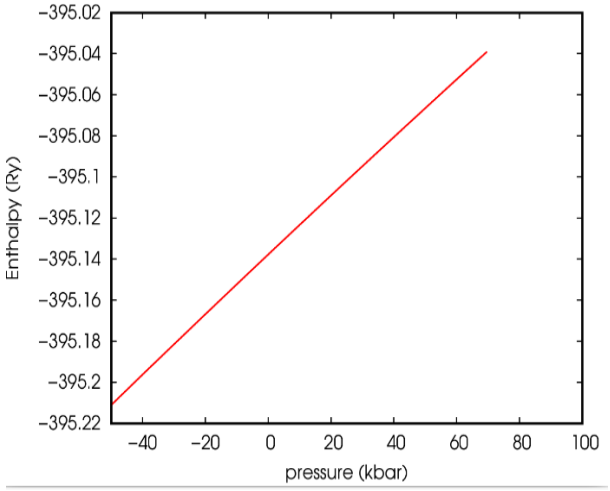

(b) enthalpy vs pressure trend visualization for rhombohedral

$LiCoO_2$. The energy minimum is located near 218–220 bohr^3 per formula unit, and the enthalpy branch evolves smoothly under compression.

This conversion is important because the value near 218 bohr^3 does not represent the full conventional cell volume in (Å)^3 rather, it is the per-formula-unit volume in atomic units.

The Birch–Murnaghan fit to the available energy–volume data gives an approximate bulk modulus of 150 – 165 GPa with B_o in the approximate range of 4.0-4.5. These values are consistent with strong Co–O bonding and the relatively low compressibility of the layered framework. Experimental high-pressure studies have reported ambient bulk moduli near this range, although numerical values vary with pressure range, fitting model, hydrostatic medium, and computational method

Figure 2(a) and (b) visualizes the energy–volume minimum and the corresponding pressure–enthalpy trend of the modeled rhombohedral branch. Because the available dataset is computed by approximate EOS parameters, the plotted curves is interpreted as trend visualizations.

*Corresponding Author: D. Yabwa

Pressure-Energy Trend

The pressure-enthalpy curve reveals that the rhombohedral R3m phase of $LiCoO_2$ remains numerically traceable and energetically well-behaved under uniform hydrostatic compression from -4 to 8 GPa, as depicted in Fig. 2(b). These results represent a controlled computational perturbation to probe intrinsic lattice stiffness, rather than a direct simulation of the complex, non-hydrostatic, and heterogeneous mechanical stresses present in operating battery cathodes

Elastic Response

The Voigt Reuss Hill elastic averages obtained from the available Thermo PW analysis (Dal Corso.2020) are summarized in Table 2. The Hill bulk modulus is 142.97 GPa, close to the EOS-derived range, while the Hill shear modulus is 44.98 GPa. The Pugh ratio $B/G = 3.18$ is above the commonly used ductile brittle threshold of 1.75. The calculated bulk, shear, and Young's moduli indicate that the investigated compound possess adequate resistance to both volume and shear deformations. The Poisson's ratios suggest that these material exhibit appreciable resistance to shear fracture at the polycrystalline average level.

Table 2: Elastic averages and mechanical indicators for layered $LiCoO_2$.

Property	Value
Hill bulk modulus, B_H	142.97 GPa
Hill shear modulus, G_H	44.98 GPa
Young's modulus, E	122.12 GPa
Pugh ratio, B_H/G_H	3.18
Poisson's ratio, v	0.358
Universal elastic anisotropy index, A_U	approximately 2.89

The elastic response is consistent with a layered oxide in which strong Co–O bonds provide resistance to volume compression, while the layered structure has anisotropic deformation pathways. The universal anisotropy index above zero indicates directional dependence in the mechanical response. Such anisotropy is important for battery cathodes applications most especially in this work because repeated lithium insertion and extraction may promote direction dependent strain accumulation and micro cracking. Nevertheless, the present elastic studies explained averaged moduli and anisotropy trends.

Debye Thermodynamic Trends

The Debye-model calculation gives a Debye temperature of approximately 680.93 K for the optimized $LiCoO_2$ structure. This relatively high value reflects stiff lattice vibrations associated with the Co–O framework (Kumar ., et al 2026, Sengar & Gupta, 2026 & Ciftci., et al 2026).The temperature-dependent Debye functions show the expected qualitative behavior which is vibrational internal energy and heat capacity increase with temperature, entropy increases as more vibrational states become thermally populated, and Helmholtz free energy decreases with increasing temperature because of the $-TS$ contribution in Eq. (3). For $LiCoO_2$, the classical Dulong–Petit limit per mole of formula. units is $3nR = 12R \approx 99.8$ J mol K because one formula units contains four atoms. Which is in agreement to computed normalized experimental Debye output (Ciftci., et al 2026). In this manuscript, the Debye model is used mainly to interpret temperature trends.

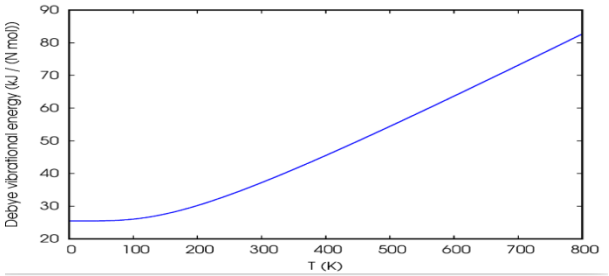

Figure 4(a): Debye Vibrational Energy Vs Temperature for $LiCoO_2$

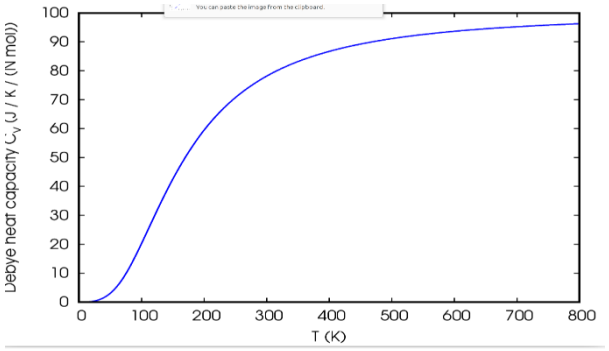

b) Debye Heat Capacity as a function of temperature for LiCoO

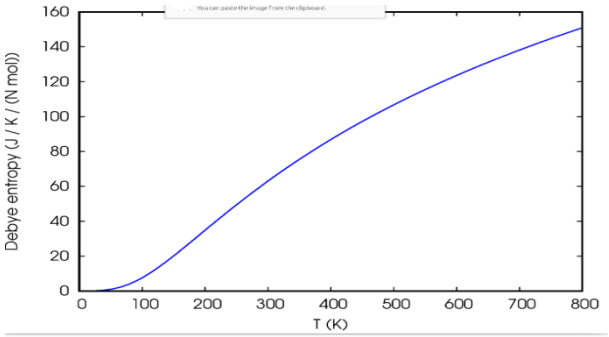

(c)Vibrational Entropy of $LiCoO_2$ as a Function of Temperature

From figure 4(a-c) provides Debye model capturing the macroscopic thermodynamic trends The analysis yields a thermodynamically consistent picture of temperature dependent increase in vibrational internal energy(a) the expected monotonic enhancement of heat capacity in (b) and vibrational entropy alongside a steady decline of the Helmholtz free energy as temperature escalates in (c). **these results indicate a thermodynamically favorable energy stability within the** Debye-Grüneisen formalism.

Implications for Cathode

The results indicate that layered $LiCoO_2$ has a compact and relatively stiff CoO_2 framework, a semiconducting electronic structure, and moderate elastic deformability at the polycrystalline averaged level. These properties are

*Corresponding Author: D. Yabwa

relevant to cathode operation because mechanical stiffness and anisotropy influence particle cracking, stress accumulation, and thermal response during cycling. The DFT+*U* result is particularly important because it gives a more realistic description of the Co 3*d* states than semi local PBE alone.

Therefore, the results stand as intrinsic materials descriptors that complement electrochemical studies, and gives extrinsic proof of improved battery safety.

Conclusions

In this work, we have conducted a comprehensive first-principles investigation of the structural, mechanical, elastic, equation of state, pressure enthalpy and Debye thermodynamic trends of $LiCoO_2$. The investigated rhombohedral compound satisfies the elastic stability criteria and exhibit energetically favorable formation characteristics within the adopted computational framework.

This study presents a first-principles assessment of layered $LiCoO_2$ using a consistent PBE and PBE+*U* framework. The optimized PBE and PBE+*U* structures give conventional hexagonal volumes of 97.37 and 97.80 $Å^3$, respectively, resolving the unit ambiguity between $bohr^3$ per formula unit and $Å^3$ per conventional cell.

The energy–volume curve has a clear equilibrium minimum, and the available Birch–Murnaghan analysis gives an approximate bulk modulus of 150–165 GPa. Elastic averages indicate a stiff but anisotropic layered lattice, with B_H = 142.97 GPa, G_H = 44.98 GPa, E = 122.12 GPa, B/G = 3.18, and ν = 0.358.

Our results give a combined effect in the pronounced intrinsic structural stiffness and stability as seen from the Debye-model thermodynamics trends where increasing vibrational energy, heat capacity, and entropy with temperature and decreasing Helmholtz free energy, our findings remain valid first principle **pass screening index to stability of $LiCoO_2$.**

CRediT authorship contribution statement

Yabwa Dlama: Writing – original draft, Software, Methodology, Formal analysis, Conceptualization. **Muhammad. A. Abdullazeez**: Writing – review & editing, Supervision. **Felix. Burari**: Writing – review & editing. **Auwal. M. Tijjani**: Writing – review & editing, Software, Methodology, Formal analysis, Conceptualization.

Declaration of competing interest

The authors declare that they have no known competing financial interests or personal relationships that could have appeared to influence the work reported in this paper.

Data availability

The data that support the findings of this study are available from the corresponding author upon reasonable request.

References

1. Asamoah, G. A., Korsah, M., Jeyasundar, P. G. S. A., Ahmed, M., Lau, S. Y., & Danquah, M. K. (2024).
2. Nanotechnology-based lithium-ion battery energy storage systems. *Sustainability*, *16*(21), 9231.
3. Choi M, Seo J, Kim MH, Kim H, Kim E, Choe J, Jang H, Ha J, Kong NJ, Kang SJ, Seo DH. Pre-disordering for Preserving Transition Metal–Oxygen covalency in Lithium-Rich Layered Oxide Cathodes. ACS Energy Letters. 2026 Feb 3.
4. Ciftci, Y. O., Durukan, İ. K., Rani, U., & Kamlesh, P. K. (2026). Phase-Dependent Structural, Optical, and thermodynamic Behavior of BaTiO 3: Insights from First-Principles Calculations. *Computers, Materials & Continua*, *87*(3), 1.
5. Cococcioni. M. and de Gironcoli. S., "Linear response approach to the calculation of the effective interaction parameters in the LDA+*U* method," *Physical Review B*, vol. 71, article 035105, 2005.
6. Dal Corso: Thermo PW. A set of fotran drivers for computation of materials properties using Quantum ESPRESSO
7. Dudarev. S. L., Botton. G. A., Savrasov. S. Y., Humphreys. C. J. and Sutton. A. P., "Electron-energy-loss spectra and the structural stability of nickel oxide: An LSDA+*U* study," *Physical Review B*, vol. 57, pp. 1505–1509, 1998.
8. Er-Rami, F. E. (2022). *Contribution to the understanding of the mechanisms involved upon cycling at high voltage of doped LiCoO2* (Doctoral dissertation, Université de Bordeaux).
9. Gao, A., Shen, S., Shang, T., Shi, Y., Zhang, H., Lin, W., ... & Gu, L. (2024). Van der Waals phase transition investigation toward high-voltage layered cathodes. *Science Advances*, *10*(33), eadp4906.
10. Giannozzi. P., Baseggio. O., Bonfà. P. Brunato. , D. Car. , R., Carnimeo. I., Cavazzoni. C., De. Gironcoli. S., Delugas. P. Ferrari Ruffino,. , F. et al., Quantum espresso toward the exascale, The Journal of chemical physics 152 (15) (2020).
11. Giannozzi. P., "Advanced capabilities for materials modelling with Quantum ESPRESSO," *Journal of Physics: Condensed Matter*, vol. 29, article 465901, 2017
12. Haq, I. U., & Lee, S. (2025). Unveiling State-of-Charge Effects on Elastic Properties of LiCoO2 via Deep Learning and Empirical Models. *Applied Sciences*, *15*(14), 7809.
13. Hu. Y. Yu,, H. Zhou,. D.. Li., F and Hu,. Z. "Structure evolution and equation of state of $LiCoO_2$ under high pressure," *Chinese Physics B*, vol. 28, article 016402, 2019
14. Jiao, S., Wang, J., Hu, Y. S., Yu, X., & Li, H. (2023). High-capacity oxide cathode beyond 300 mAh/g: focus review. *ACS Energy Letters*, *8*(7), 3025-3037.

*Corresponding Author: D. Yabwa

15. Koech, A. K., Mwandila, G., Mulolani, F., & Mwaanga, P. (2024). Lithium-ion battery fundamentals and exploration of cathode materials: A review. *South African Journal of Chemical Engineering*, *50*(1), 321-339.
16. Lambert, D. S., & O'Regan, D. D. (2023). Use of DFT+ U+ J with linear response parameters to predict non-magnetic oxide band gaps with hybrid-functional accuracy. *Physical Review Research*, *5*(1), 013160.
17. Maran, T., Jain, A., Sundaramoorthy, M., Roy, A. P., Joseph, B., Lingannan, G., ... & Sonachalam, A. (2024). Hydrostatic pressure effect on structural and transport properties of co-existing layered and disordered rock-salt phase of Li x CoO 2. *Physical Review Materials*, *8*(12), 125401.
18. Nitta, N. F. Wu, J. T. Lee and G. Yushin, "Li-ion battery materials: Present and future,"*Materials Today*, vol. 18, pp. 252–264, 2015.
19. Osemeikhian, O. (2017). *Sol-gel and solid-state fluorination of lithium cobalt oxide for Li-ion secondary batteries* (Master's thesis, University of Pretoria (South Africa)
20. Patel, A. (2025). Development, Synthesis and Characterization of Advanced Low-Cobalt and High-Nickel Cathode Materials for Lithium-Ion Batteries.
21. Perdew. J. P., Burke. K. and Ernzerhof. M., "Generalized gradient approximation made simple, *Physical Review Letters*, vol. 77, pp. 3865–3868, 1996.
22. Rahman, A., Ahmad, S., Abderrazek, O., Zhou, Z., & Saheb, N. (2026). First-principles study of dual-site Sr–M (M= Ga, Hf, Ge) co-doping in the perovskite solid electrolyte Li0. 5La0. 5TiO3: effects on Li+ migration and electronic insulation. *Journal of Materials Chemistry A*.
23. Raman, M. (2026). *Hubbard-Corrected Density Functional Theory: Sensitivity to Projection-Space and Renormalization of Coulomb Interaction* (Doctoral dissertation, Baylor University).
24. Romanova, A. D., Boev, A. O., Savina, A. A., & Abakumov, A. M. (2026). Single-crystal layered oxides as cathode materials for next-generation lithium-ion batteries. *RUSSIAN CHEMICAL REVIEWS*, *95*(5).
25. Sengar, S. S., & Gupta, D. C. (2026). Structural, electronic, transport and thermodynamic Properties of layered rare-earth nickelates: a first-principles study relevant to nuclear materials. *Journal of Nuclear Materials*, 156667.
26. Shi Y, Hu E, Sumboja A, Anggraningrum IT, Syahrial AZ, Yan Q. Layered 3d Transition Metal-Based Oxides for Sodium-Ion and Lithium-Ion Batteries: Differences, Links and Beyond. Advanced Functional Materials. 2025 Jan;35(2):2413078.
27. Tang, H., Zheng, Y., Wang, Y., Feng, L., Du, H., & Li, B. (2026). Advancements in cathode materials for lithium-ion batteries: Mechanism innovations, multiscale characterization, and data-driven design. *Nano Research*.
28. Wang. L., Maxisch. T. and Ceder. G., "Oxidation energies of transition metal oxides within the GGA+*U* framework," *Physical Review B*, vol. 73, article 195107, 2006.
29. Wang, L., Chen, B., Ma, J., Cui, G., & Chen, L. (2018). Reviving lithium cobalt oxide-based lithium secondary batteries-toward a higher energy density. *Chemical Society Reviews*, *47*(17), 6505-6602.
30. Wang. X., Li. H., Huang. X., Baudrin. E. and Chen. L., "Effect of pressure on structural properties and Raman modes of $LiCoO_2$," *Physical Review B*, vol. 72, article 224102, 2005.
31. Wu, S., Zhao, T., Lan, D., Sun, J., Zhang, X., Liu, D., ... & Zhao, Z. (2026). A Panoramic Review on Intercalation-Based Electrochemical Lithium Extraction from Salt Lakes: Mechanisms, Challenges, and Optimization Strategies. *Advanced Materials*, *38*(33), e73237.
32. Wu, S., Chen, Y., Luan, W., Chen, H., Huo, L., Wang, M., & Tu, S. T. (2024). A review of multiscale mechanical failures in lithium-ion batteries: implications for performance, lifetime and safety. *Electrochemical Energy Reviews*, *7*(1), 35.
33. Yu D, Zeng G, Chen D, Yan Y, Zou Y, Liu Q, Zhang K, Fang K, Xu J, Yin W, Hong YH. Revealing gliding-induced structural distortion in high-nickel layered oxide cathodes for lithium-ion batteries. ACS nano. 2024 Sep 26;18(40):27654-64.
34. Zhou. F. Cococcioni., M., Marianetti. C. A., Morgan. D and Ceder. G, "First-principles prediction of redox potentials in transition-metal compounds with LDA+*U*," *Physical Review B*, vol. 70, article 235121, 2004.

*Corresponding Author: D. Yabwa